

令和元年6月25日現在

機関番号：14301
研究種目：若手研究(B)
研究期間：2017～2018
課題番号：17K14571
研究課題名(和文) Micro-bubble assisted abrasive waterjet polishing

研究課題名(英文) Micro-bubble assisted abrasive waterjet polishing

研究代表者

ブカン アントニー (Beucamp, Anthony)

京都大学・工学研究科・講師

研究者番号：30756838

交付決定額(研究期間全体)：(直接経費) 3,400,000円

研究成果の概要(和文)：The mechanism of material removal boosting in ultrasonic fluid jet polishing was investigated. Macro-scale fluid vibrations were found to cause increased erosive action by abrasive particles. The fundamental understanding of this novel process opens the door to optical and medical applications.

研究成果の学術的意義や社会的意義

Fluid jet polishing is a very flexible method for polishing small and complex surfaces, such as aspheric lenses for smartphones or dental implants, but was however inefficient. With this research, the productivity of FJP was greatly enhanced, which will benefit consumers of such important products.

研究成果の概要(英文)：In fluid jet polishing (FJP), a polishing liquid is pressurized as a jet and impinges a surface. An improved system consisting of an ultrasonic transducer and acoustic lens mounted atop the FJP nozzle cavity was tested, which boosted material removal rates by up-to 1000%. However, it was not clear whether the removal boost was due to a micro-scale or macro-scale phenomenon.

A study of micro-pit formation by collapsing micro-bubbles in the near wall region determined that micro-jetting and water hammer pressure do not seem to occur in UFJP, so the micro-scale hypothesis was ruled out.

A study of workpiece vibrations found that significant shear forces exist at the workpiece surface when ultrasonic vibration is applied to the FJP beam. After theoretical confirmation of the correlation between macro-scale fluid displacement and shear force, the standard erosion model in FJP was modified by adding time-averaged vibration terms. The model and experiments were finally in good agreement.

研究分野：マイクロエンジニアリング(工学)

キーワード：ultra-precision fluid jet polishing ultrasonic cavitation material removal surface finishing optical surfaces medical surfaces

様式 C - 19、F - 19 - 1、Z - 19、CK - 19 (共通)

1 . 研究開始当初の背景

Fluid Jet Polishing (FJP) is a flexible process for super-fine finishing of small and complex workpiece geometries. A slurry of loose abrasives and carrier fluid is pressurized and pushed out through a nozzle orifice 0.1 to 1.0 mm in diameter, generating a narrow fluid beam. Impingement of the beam onto a workpiece surface results in a sub-millimeter footprint of time dependent material removal. The principal advantages of FJP include lack of tool wear, ease of access to deeply recessed areas, and the ability to reach nanometer-level surface finish on various materials.

However, as compared to micro-waterjet machining, relatively benign processing pressure and abrasive grain size are necessary to achieve smooth polishing in FJP. This results in generally low material removal rate, and long processing time for larger surfaces. To address this issue, an enhancement was proposed in the form of Ultrasonic cavitation assisted FJP (UFJP). The principle is shown in Fig. 1: an ultrasonic transducer is fitted with an acoustic lens and mounted at the top of a conical cavity. The focal point of acoustic pressure waves coincides with the outlet of the nozzle, where micro-bubbles are generated by cavitation. When compared to standard FJP, the novel process was found to significantly increase material removal rate by a factor of up-to 1000%. Furthermore, the final surface roughness was maintained or even slightly improved, a result in sharp contrast with other FJP enhancement systems such as air-bubble injection.

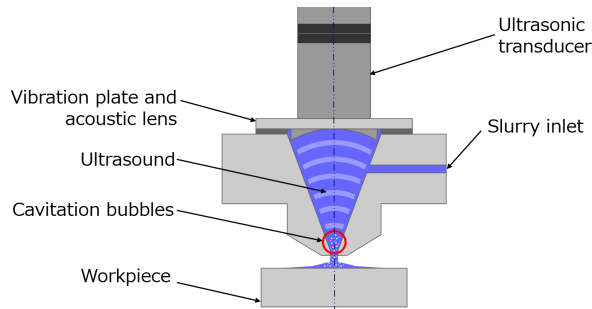


Figure 1. Principle of ultrasonic cavitation assisted FJP

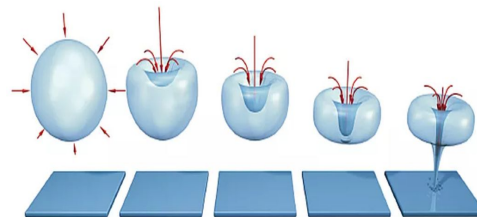


Figure 2. Principle of micro-bubble collapse near a wall

Ultrasonic cavitation promotes the formation and growth of micro-bubbles within water, especially in cases where air or other gases are dissolved in the fluid. In cases where such micro-bubbles come near a surface wall (at a distance approximately equal to their diameter), the likelihood of collapse increases due to asymmetric redistribution of surface tension. Fig. 2 shows the principle of micro-bubble collapse near a surface wall: the top side caves-in and a micro-jet punches through the bubble and lurches towards the wall. Micro-jet velocities typically in the range 100 - 500 m/s have been recorded experimentally. Such high fluid displacement velocities result in the so-called water-hammer effect, which causes micro-pit damage to the wall. In cavitation experiments on aluminum sheets, measured micro-pit have diameters in the range 4 - 14 μm and depths in the range 0.06 - 0.88 μm .

2 . 研究の目的

In this research, the process mechanism in UFJP was investigated in order to establish the fundamental phenomenon driving the material removal rate boost observed in experimental trials, and understand the influence of the various process parameters. Two possible hypotheses were proposed for the nature of the process mechanism:

(a) the mechanism occurs at the micro-scale due to micro-bubble collapse near the workpiece surface. In the micro-scale hypothesis for the UFJP mechanism, it is theorized that micro-jetting of the surface by collapsing bubbles results in a combination of strain hardening of the workpiece material and sudden energizing of abrasive particles entrained in the water-hammer zone. Both of these effects would promote a higher removal rate in the regions influenced by micro-jetting.

(b) the mechanism occurs at the macro-scale due to vibration of the polishing fluid in the impingement zone. **In the macro-scale hypothesis, the increase in material removal rate is theorized to issue from additional erosive action of the abrasive particles due to vibrations of the body of slurry in the zone of UFJP impingement. Such vibrations may come from two related sources: (1) a fraction of the acoustic pressure waves escaping the nozzle cavity through the outlet instead of being reflected, and (2) the generation of shock waves at the nozzle outlet due to the periodic switching between disparate densities and dynamic viscosities of the ejected fluid, in the form of slurry and slurry/micro-bubble mixture.**

Each hypothesis was investigated through experimental trials, in order to qualify the more likely explanation. Thereafter, a theoretical model of the removal mechanism was proposed that builds upon the generally accepted material removal model for standard FJP, but introduces new parameters accounting for the influence of ultrasonic acoustic waves. Finally, prediction from the model were verified against experimental material removal footprint data.

3 . 研究の方法

To verify the micro-scale hypothesis, experiments were carried out in which pure water only was injected into the cavitating nozzle (e.g. no abrasives). Optical glass mirrors coated with a layer of aluminum several hundred microns thick were measured by a whitelight interferometer with 50x magnification objective, at the same location before and after processing by the ultrasonic water jet. Experimental conditions are

summarized in Table 1. A control experiment was carried out by placing some of the aluminum coated mirrors into an ultrasonic bath cleaning unit, of similar operating frequency to the UFJP system. The system consists of a tank below which 2 transducers of 50W each are mounted. The samples were suspended in water 67 mm above the bottom of the tank, along the axis of one of the transducers. This control experiment was conducted in order to ensure that micro-pits are indeed generated on the aluminum through the dielectric overcoat, for a power (50 W) and distance (50-60 mm) between transducer and workpiece equivalent to the UFJP setup.

To verify the macro-scale hypothesis, experiments were carried out in which pure water only was injected into the cavitating nozzle (e.g: no abrasives). The UFJP beam was impinged onto an aluminum block affixed to a 3-axis dynamometer, and the force was recorded with a 1 MHz data logger. A control experiment at 0 MPa was carried out to establish the influence of structural vibration from the experimental jig. Experimental conditions are summarized in Table 2.

Table 1.
Parameters of micro-jet experiment

Workpiece <ul style="list-style-type: none"> • Dimensions • Substrate material • Coating material • Surface roughness • Exposure time 	25 x 25 x 3 mm Float glass Aluminum with dielectric overcoat Ra <2 nm 60 min
Ultrasonic FJP <ul style="list-style-type: none"> • Operating frequency • Input power • Nozzle diameter • Pump pressure • Workpiece distance • Working fluid 	22 kHz 50 W (focused on impingement zone) 1 mm 0.4 MPa 3 mm (outlet) / 53 mm (transducer) Pure water
Control Experiment <ul style="list-style-type: none"> • Device • Bath dimensions • Operating frequency • Input power • Workpiece distance • Working fluid 	Ultrasonic bath cleaner 150 x 75 x 50 mm 28 kHz 2 x 50W 67 mm (transducer) Pure water

Table 2.
Parameters of macro-vibration experiment

Workpiece <ul style="list-style-type: none"> • Dimensions • Substrate material • Surface roughness 	40 x 40 x 15 mm Aluminum Ra 0.18 μ m
Ultrasonic FJP <ul style="list-style-type: none"> • Operating frequency • Input power • Nozzle diameter • Nozzle distance • Pump pressure • Working fluid 	22, 71, 127 kHz 50 W 1 mm 3 mm 0, 0.2, 0.4, 0.8 MPa Pure water
Dynamometer <ul style="list-style-type: none"> • Device • Pre-load • Sampling rate 	3-axis (Kistler 9027C) 14 kN 1 MHz

3.1 Micro-scale hypothesis

The workpieces processed in the control experiment featured numerous micro-pits across the entire surface, and hotspots of higher micro-pit density. Fig. 3(a) and 3(b) show the same area of a workpiece before and after processing, with the appearance of a dozen larger, and another dozen smaller micro-pits. **At hotspots of activity on the surface, over 50 micro-pits in the range 1 to 4 μ m in diameter, and 0.04 to 0.09 μ m in depth, could be observed.** By comparison, there was a thorough lack of micro-pit on the surface of all samples processed by water only UFJP. In a series of measurements taken at 1 mm intervals from the centre to the edge of the jet impingement zone, the height range for this measurement, between -2 and 12 nm, confirms that no micro-pits are present on the surface.

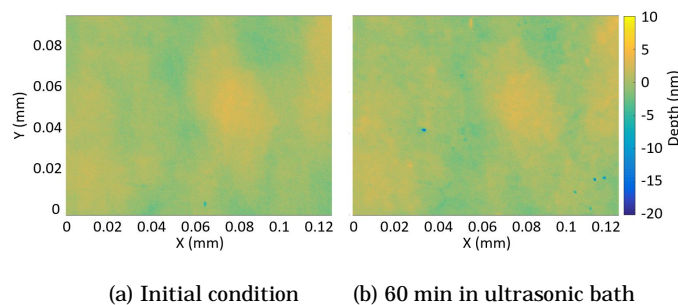


Figure 3. Observations of workpiece processed in control experiment

From the absence of micro-pits on the UFJP processed samples, it is assumed that micro-jetting of the surface by micro-bubbles either did not occur in the impingement region, or that the water-hammer pressure was so negligible that plastic deformation of the aluminum coating did not occur. In the first case, the most plausible explanation is that micro-bubbles cannot penetrate the near-wall fluid shear layer, and simply follow fluid streams in the layer above. In either case, it may be safely assumed that micro-jetting is not a major factor influencing the material removal mechanism in UFJP. Consequently, the micro-scale hypothesis may be considered as the least likely explanation for the increased removal rate in UFJP.

3.2 Macro-scale hypothesis

Control experiments at 0 MPa showed that a very low amplitude signal is transferred from the nozzle to the workpiece through structural vibration of the experimental jig. However, this signal was

negligible when compared to signals transferred through the fluid jet.

Fig. 4 shows typical results of force measurements in the lateral and normal directions, after subtraction of the DC component. While almost no vibration of the force was detected in standard FJP, vibrations of magnitude 0.5 – 2.0 N were detected at all operational frequencies of the ultrasonic FJP system. The strongest vibrations were recorded at 22 kHz, which is also the frequency producing the strongest material removal boost (see Fig. 2). Spectral analysis of the signals by Fourier transform revealed a strong peak at 22 kHz when using the associated frequency. Peaks at 71 and 127 kHz were less pronounced, as these frequencies are beyond the specification range of the dynamometer used in this experiment. A low frequency peak at 50 Hz was detected in all measurements, including standard FJP, and is assumed to relate to pulsations of the slurry pressuring system. From these experiments, compelling evidence of fluid vibration being transferred to the workpiece surface was detected. Consequently, the macro-scale hypothesis was selected as a basis on which to build a model of material removal in UFJP.

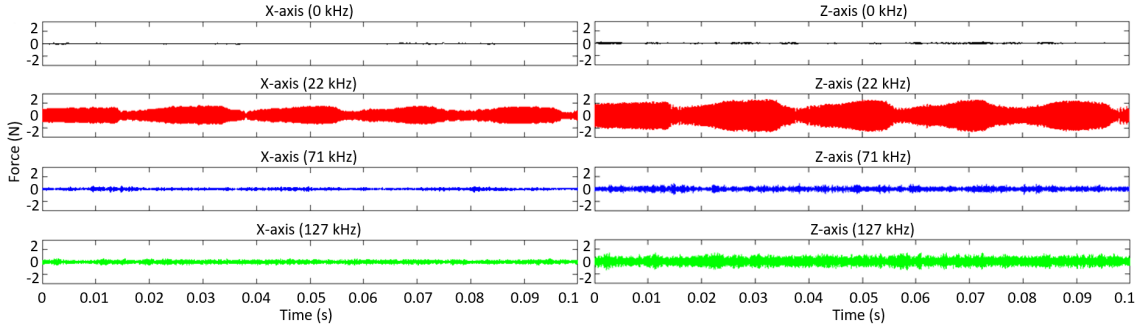


Figure 4. Workpiece vibration force when subjected to standard and ultrasonic FJP at 0.8 MPa pressure

3.3 Fluid displacement and shear force

Computational Fluid Dynamics (CFD) simulations were carried out in order to determine the correlation between vibratory fluid displacement and wall forces in the impingement area of the UFJP beam. The time dependent displacement $x(t)$ [m] can be expressed as function of the amplitude A [mm] and frequency f [Hz]:

$$x(t) = A \sin(2\pi ft) \quad (1)$$

By application of Newton's second law of motion on a body of fluid of density ρ [kg/m³], the equivalent force per unit of volume $F_{V,x}$ [N/m³] can be expressed as:

$$F_{V,x} = \rho \frac{d^2 x}{dt^2} = -\rho A (2\pi f)^2 \sin(2\pi ft) \quad (2)$$

CFD model conditions in the case of lateral vibration are shown in Fig. 5. The fluid is surrounded by a slip wall at the top (water/air boundary), open boundaries on the sides, and no-slip wall at the bottom (water/workpiece boundary). Mesh density was increased in the region close to the workpiece surface, and a boundary probe added to assess the shear stress.

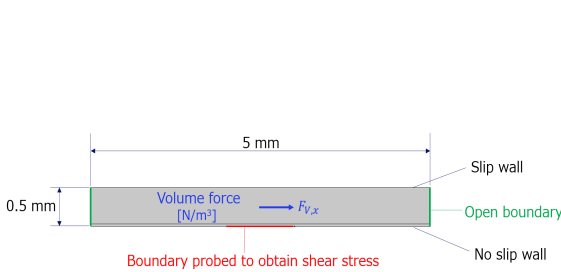


Figure 5. CFD model conditions for fluid/wall interaction

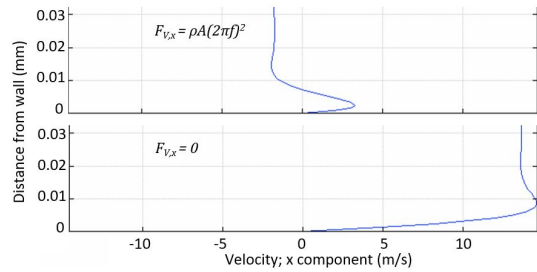


Figure 6. Velocity profile vs. body force ($A=0.1\text{mm}$, $f=22\text{kHz}$)

Fig. 6 shows fluid displacement velocity profiles in the near wall region, at the maximum and minimum of body force oscillations. Abrasive particles in the micron size range must be strongly affected by these 10 m/s scale fluctuations of the fluid velocity. The correlation between total shear force and maximum fluid displacement velocity is shown in Table 3. The amplitude was rescaled as function of the operating frequency, in accordance with the actual power output of the ultrasonic generation equipment. Simulations were found to agree reasonably well with the experimental measurements of the total shear force.

Table 3.

Correlation between fluid displacement and shear force

Conditions	Fluid velocity	Shear force
A = 0.2 mm, f = 22 kHz	27.6 m/s	0.72 N
A = 0.1 x (22/71) x √0.5 mm, f = 71 kHz	9.77 m/s	0.41 N
A = 0.1 x (22/127) x √0.25 mm, f = 127 kHz	6.91 m/s	0.36 N
Standard FJP at 0.8 MPa (surface average)	5.0 m/s	0.29 N

3.4 Modified erosion model for ultrasonic FJP

A comprehensive model of material erosion in standard FJP was proposed in the literature. Considering the impact of a single abrasive particle on the surface with tangential velocity v_x [mm/s] and normal velocity v_z [mm/s], the volume of eroded material V [mm³] is expressed as:

$$V = k \left(\frac{1}{2} m_p v_x^2 \right) \left(\frac{1}{2} m_p v_z^2 \right)^{\frac{2(1-b)}{3}} \quad (3)$$

where m_p [kg] is the abrasive particle mass, k a material depend coefficient accounting for plastic flow pressure and material spring back, and b ($0.5 \leq b \leq 1$) a material depend exponent of the cross-section area of abrasive indentation.

Using CFD simulations of the jet plume and abrasive particle tracing, the abrasive grains velocity and density $\sigma_a(r)$ [1/mm²s] as function of radial distance from the impingement centre can be used to compute the overall material removal footprint $E(r)$ [mm/s]:

$$E(r) = \sigma_a(r) V(v_x(r), v_y(r)) \quad (4)$$

In order to account for the influence of fluid vibrations in the impingement region of an ultrasonic cavitation assisted FJP beam, a modification of Cao's model is proposed by introducing the time-average of vibrations with velocity magnitude $v_{x,vib}$ and $v_{z,vib}$ [mm/s] into the single abrasive removal equation (3):

$$V = k \left(\frac{1}{2} m_p (v_x^2 + \frac{1}{2} v_{vib,x}^2) \right) \left(\frac{1}{2} m_p (v_z^2 + \frac{1}{2} v_{vib,z}^2) \right)^{\frac{2(1-b)}{3}} \quad (5)$$

The vibration velocity magnitude is expressed as function of the radial distance r from the centre of the impingement region. To test the validity of this modification, removal profiles were computed for two different distributions of vibration velocity, as shown in Fig. 7. The corresponding experimental conditions were: 4 μ m Al₂O₃ particles at 20 g/L, 0.8 MPa pressure, 26 kHz frequency and 50 W power. In case (a), a plateau distribution represents coordinated vibration of the entire impingement zone. In case (b), a ring distribution signifies exclusion of the fluid stagnation region at centre of the impingement area. Simulated removal profile were found to match reasonably well the experimental data for case (b), indicating that vibrations must be dampened in the stagnation region.

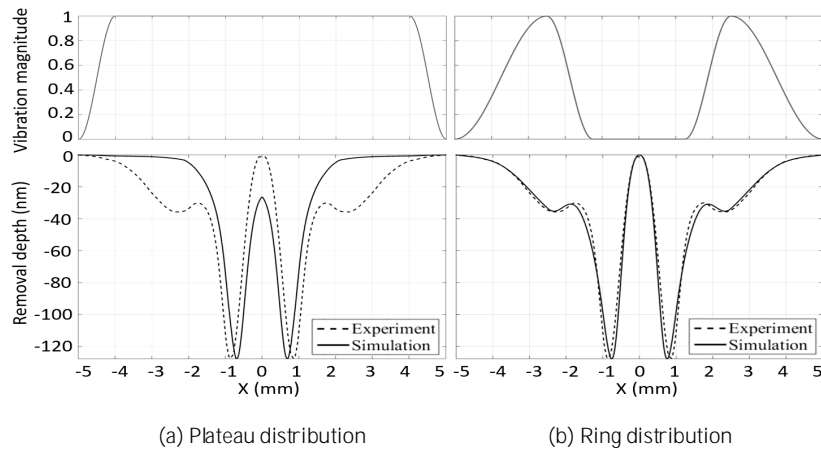


Figure 7. Comparison of experimental and simulated material removal for two distributions of the vibration magnitude

4 . 研究成果

FJP is a very flexible finishing method that suffered from low material removal rates until a novel system consisting of an ultrasonic transducer and acoustic lens mounted atop the nozzle cavity was proposed, through which removal rates can be boosted by up-to 1000%. In this research project, the process mechanism was investigated to determine whether a micro-scale or macro-scale phenomenon underlies the boost in material removal rate.

A study of micro-pit formation by collapsing micro-bubbles in the near wall region determined that micro-jetting and water hammer pressure do not seem to occur in UFJP. Consequently, the micro-scale

hypothesis was ruled out as unlikely.

A study of workpiece vibrations found that significant shear forces exist at the workpiece surface when ultrasonic vibration is applied to the FJP beam, caused by periodic displacement of the body of fluid in the impingement region. After theoretical confirmation of the correlation between fluid displacement and shear force, a modification of the erosion model for standard FJP was proposed in the form of time-averaged vibration velocity terms, and was verified against experimental removal footprint data. The model and experiments were in reasonable agreement.

Future work would involve experimentally ascertaining that the relative vibration magnitude matches a ring distribution, though arrays of 3-axis force sensors are not sufficiently miniaturized to realize such experiment at the time of this research.

5 . 主な発表論文等

〔雑誌論文〕(計6件)

- (1) W. Zhu, S. Ben Achour, **A. Beaucamp**: Centrifugal and hydroplaning phenomena in high-speed polishing. *CIRP Annals*, **68/1** (2019) accepted for publication
- (2) W. Zhu, **A. Beaucamp**: Ultra-precision finishing of low expansion ceramics by compliant abrasive technologies: A comparative study. *Ceramics International*, **45/9** (2019) pp. 11527-11538
- (3) D. Walker, G. Yu, H. Li, B. Myer, **A. Beaucamp**, Y. Namba, L. Wu: Title advances in optical fabrication for astronomy, *Monthly Notices of the Royal Astronomical Society*, **485/2** (2019) pp. 2017-2082
- (4) **A. Beaucamp**, T. Katsuura, K. Takata: Process mechanism in ultrasonic cavitation assisted fluid jet polishing, *CIRP Annals*, **67/1** (2018) pp.361-364
- (5) Y. Han, L. Zhang, C. Fan, W. Zhu, **A. Beaucamp**: Theoretical study of path adaptability based on surface form error distribution in fluid jet polishing. *Applied Sciences*, **8/10** (2018) pp.1814
- (6) K. Takizawa, **A. Beaucamp**: Comparison of tool feed influence in CNC polishing, between a novel circular-random path and other pseudo-random paths, *Optics Express*, **25/19** (2017) pp.22411

〔学会発表〕(計5件)

- (1) **A. Beaucamp**, W. Zhu, H. Robbins: Fabrication of ultraprecise silicon mirror by shape adaptive grinding and bonnet polishing, Proc. JSPE (2019)
- (2) M. Ihara, **A. Beaucamp**, A. Matsubara: Modelling of zero-velocity point removal in polishing, Proc. JSPE (2018)
- (3) T. Katsuura, **A. Beaucamp**: Characterization of ultrasonic cavitation assisted fluid jet polishing, Proc. JSPE (2017)
- (4) K. Takizawa, **A. Beaucamp**: Comparison of tool feed influence in CNC polishing with several pseudo-random paths, Proc. JSPE (2017)
- (5) M. Ihara, **A. Beaucamp**: A. Matsubara, Servo tuning method and process simulation for CNC polishing machine, Proc. JSPE (2017)

〔図書〕(計1件)

- (1) Micro & Nano Fabrication Technology: Micro-fluid jet polishing, Springer (2018)

〔産業財産権〕

出願状況(計0件)

取得状況(計0件)

〔その他〕

ホームページ等: N/A

6 . 研究組織

(1)研究分担者

研究分担者氏名:

ローマ字氏名:

所属研究機関名:

部局名:

職名:

研究者番号(8桁):

科研費による研究は、研究者の自覚と責任において実施するものです。そのため、研究の実施や研究成果の公表等については、国の要請等に基づくものではなく、その研究成果に関する見解や責任は、研究者個人に帰属されます。